Notched response of OSB wood composites

Paolo Feraboli *

Department of Aeronautics and Astronautics, University of Washington, P.O. Box 352400, Seattle, WA 98195-2400, United States

ARTICLE INFO

ABSTRACT

Oriented strand board (OSB) is a form of wood composite manufactured from long, narrow strands bonded together with resin under heat and pressure. A large experimental database is gathered here that shows that OSB can be considered a notch-insensitive material thanks to its heterogeneous nature. Notched tensile strength does not decrease with hole size for hole diameters tested, and that for low to moderate hole sizes failure often occurs in the gross section away from the hole. The existence of an intrinsic material stress concentration is suggested, based on the existence of a constant characteristic dimension, and probabilistic considerations are used to gain insight on the observed behaviors. Scaled-up unnotched and notched specimens tend to fail at lower applied stress, but follow similar overall behavior.

1. Introduction

Wood, a naturally occurring fibrous composite material, has been a construction material by choice for centuries, even for early airframes. However, because wood properties vary between species, between trees of the same species, and between pieces from the same tree it is difficult to obtain consistent and repeatable products with solid wood. Still nowadays, material and process control is the main force preventing broader use of bio-based composites. When processing variables are properly selected, engineered wood materials, also known as wood composites, can surpass natural wood as structural materials. With solid wood, changes in properties are studied at the cellular level, while for engineered wood materials, they are studied at the fiber, particle, strand, or veneer level. Properties of such materials can be tailored to specific applications by combining, reorganizing, or stratifying these elements. Conventional wood composites are grouped into two general categories: plywood, and other wood composites, which include oriented strandboard (OSB), particleboard, and fiberboard [1].

Plywood is a flat panel built up of plies of veneer joined by a thermoset adhesive (usually phenolic resin), and consolidated under heat and pressure to create a laminated panel. Plywood is constructed of layers with the grain direction oriented perpendicular to one another, which provides it with similar axial strength and stiffness properties in perpendicular directions within the panel plane. Plywood has been successfully used in engineering application that needs high quality sheet material, and for decades it has provided the benchmark for wood-based construction materials.

Although plywood is by all means a wood composite, the term wood composites is usually reserved to the other three family of materials, which employ finite-sized reconstituted reinforcements. All the products in the family of wood composite materials are processed in similar ways. Raw material for oriented strandboard, particleboard and fiberboard is obtained by flaking or chipping lumber. The chopped wood is then dried, adhesive is applied, and a mat of wood particles, fibers, or strands is formed; the mat is then pressed under heat until the adhesive is cured. Particleboard is produced by mechanically reducing the wood processing byproducts, such as sawdust, into small particles, and is generally not used for structural applications because of its lower mechanical performance. Fiberboard, which includes hardboard and medium-density fiberboard (MDF), is comprised of longer lignocellulosic fiber bundles randomly oriented in a three-dimensional mat. Fiberboard exploits the inherent strength of wood to a greater extent than does particleboard, and is therefore used in more structural applications, such as furniture [2]. Another recent member of the wood composites family is oriented strandboard (OSB), which is an engineered structural panel manufactured from long, narrow strands, which have a typical aspect ratio (length divided by width) of at least three [1], and are typically several inches in length (Fig. 1).

Since its debut in the early 1980s, OSB has virtually replaced other panels in new residential construction in North America. OSB is typically used in large sheets for roof, wall, and floor sheathing, for which the OSB Design Manual [3,4] contains guidelines that range from rated span to nail and screw patterns. OSB has nearly tripled its share of the North American structural sheathing market to 70%, and production of OSB overtook that of plywood in the year 2000 for the first time. Today, all building codes in the US and Canada recognize OSB panels for the same uses as plywood on a thickness-by-thickness basis.

* Tel.: +1 11 206 543 2170; fax: +1 11 206 543 0217.
E-mail address: feraboli@aa.washington.edu

Fig. 1. Examples of baseline OHT specimens and scaled-up specimens with various hole diameters.

In general OSB can be manufactured at a significantly lower cost than plywood, and yet it exhibits mechanical performance similar to that of plywood, see Table 1 [1,3,4]. In general, shear and tensile strengths are consistently lower than compressive and flexural strengths. While the literature on OSB is rather limited, the majority of the efforts in the area have been limited to studying the influence of the stand distribution on the material properties, and how such distribution can be monitored and controlled to improve the quality of the manufacturing process [5–14]. Several approaches have been proposed for inferring the mechanical performance of OSB panels by indirect measurements.

Moses et al. [15] uses laminate theory and Tsai-Wu failure theory, typically used for advanced polymer composites, to predict the elastic and failure behavior of laminated strand lumber (LSL). LSL differs from OSB for the longer and thicker strand dimensions, and the typically greater panel (laminate) thickness. More importantly, LSL is usually available with specific strand orientations, from unidirectional (0°) to cross-ply (0/90°). The study characterizes the effect of five stacking sequences on tensile, compressive, and shear properties, and in particular the study investigates the response of fully aligned, completely random, and three intermediate combinations. The study mentions a possible size effect related to the length of the test specimen in tension, observed while testing two different specimen dimensions, but does not address it explicitly.

This study investigates specifically the notched failure response of OSB, in particular the tensile strength of specimens containing circular holes of a various dimensions, and the influence of specimen size and scaling on the measured strength.

2. Experimental set-up

The material used for the investigation is commercially available 3/8-in. thick (0.375 in. or 9.5 mm) sheathing-grade OSB. Sheets of the same nominal thickness and average measured thickness of 0.40 in. (10 mm) are employed during this investigation.

The specimen used to measure open-hole tensile (OHT) as well as unnotched tensile (UNT) strengths is based on the SACMA SRM-5 recommended test method [16] for advanced polymer composites. The specimen is a straight-edged, untabbed rectangular plate indicated as family A in Table 2, whose baseline dimensions are 8 in. × 2 in. (203 mm × 51 mm). Keeping a constant length/width aspect ratio (Fig. 1), the effect of specimen width is investigated to isolate possible effects associated with the finite length scale of the wood strands. Scaled-up specimens, indicated as families B, C and D, respectively, having geometry 12 in. × 3 in. (305 mm × 76 mm), 16 in. × 4 in. (406 mm × 102 mm), and 32 in. × 8 in. (813 mm × 203 mm), are also tested while keeping all other parameters constant. Although the distribution of strand lengths in a panel is rather large with peaks of 6.0 in. (152 mm), the average length of the surface strands on the panels investigated is approximately 3.0 in. (76 mm). Thus an 8-in. test gage (203 mm) width offers over 2.5 times the length of the nominal strand. The baseline specimen configuration is used to perform the bulk of the investigation, both in terms of total specimens tested and number of D/W ratios investigated. Due to the high variation in measured strength associated to these natural materials, over hundred specimens are tested for the baseline configuration. Details on the test matrix are reported in Table 2.

Table 2
Test matrix, with varying hole diameter and specimen width

Family	Width (W) (in.)	Length (L) (in.)	Thickness (t) (in.)	Hole diameter (D) (in.)	D/W	Number of repetitions (N)
A	2	8	0.4	0.000	0.000	24
A	2	8	0.4	0.125	0.063	24
A	2	8	0.4	0.250	0.125	24
A	2	8	0.4	0.375	0.188	24
A	2	8	0.4	0.500	0.250	24
A	2	8	0.4	0.625	0.313	24
A	2	8	0.4	0.750	0.375	24
B	3	12	0.4	0.000	0.000	10
B	3	12	0.4	0.600	0.200	10
B	3	12	0.4	0.750	0.250	10
B	3	12	0.4	0.900	0.300	10
B	3	12	0.4	1.000	0.333	10
C	4	16	0.4	0.000	0.000	10
C	4	16	0.4	0.250	0.063	10
C	4	16	0.4	0.500	0.125	10
C	4	16	0.4	1.000	0.250	10
C	4	16	0.4	1.500	0.375	10
D	8	32	0.4	0.000	0.000	10
D	8	32	0.4	0.500	0.063	10
D	8	32	0.4	1.000	0.125	10
D	8	32	0.4	2.000	0.250	10
D	8	32	0.4	3.000	0.375	10

Table 1
Comparison between typical material properties of plywood and OSB, based on [1]

Property	Plywood	OSB
Flexure strength (ksi)	3.0–7.0	3.0–4.0
Tensile strength (ksi)	2.0–4.0	1.0–3.0
Compressive strength (ksi)	3.0–5.0	1.5–4.0
Shear strength thru-thickness (ksi)	0.6–1.1	1.0–1.5
Shear strength in-plane (ksi)	0.2–0.3	0.2–0.3
Modulus (Msi)	1.0–2.0	0.7–1.2
Shear modulus (Msi)	0.2–0.3	0.2–0.5

Specimens are machined to the required width and length from stock 4 ft × 8 ft (1.2 m × 2.4 m) sheets using a table saw, and then drilled for the desired hole size. The edges of each sheet are trimmed by 3 in. (76 mm) on each side to eliminate the outermost portion of the material that may not be in pristine condition. Specimens are tested at room temperature without prior desiccation. Gripping is performed with purposely designed grips that feature tapered geometry and serrated surface that facilitate progressive introduction of the load and, after several trials and revisions, virtually eliminated all grip failures (when failure occurs in proximity of the grip rather than in the test gage). Testing is performed in a 67,400 lb (300 kN), high-stroke electromechanical test frame, under displacement control.

It should be noted that density has been proved to greatly affect the strength of wood composites, and given the high variation that can be encountered in a panel, it is possible that such variation may be responsible for a substantial part of the variability observed in the results. Future research should ensure that the density of each specimen is assessed prior to testing, and that strength results be normalized but individual specimen density. Using density as a covariate when analyzing the unnotched and notched results would contribute in reducing some of the observed scatter.

Another known contributor to variability in strength of wood composites is moisture, and it the degree of moisture absorption and swelling in each test specimen can lead to decreased measured strength. Future research should also ensure that each specimen is dried in an oven at moderate temperatures to remove excess moisture and further increase the level of consistency in the physical state of the specimen prior to testing.

3. Results and discussion

When calculating the OHT strength of composite materials, where stress concentration factors depend on the stacking sequence and local stress state in the vicinity of the notch is not as clearly defined due to the heterogeneity of the material, two approaches can be used. The first calculates the notched σ_N^{OHT} strength of the material as the maximum sustained load P divided over the net section $(w - d)$, and is defined as

$$\sigma_N^{OHT} = \frac{P}{(w - d) \cdot t} \tag{1}$$

where w is the width of the specimen and d is the hole diameter, while t is the specimen thickness. The other approach employs the gross strength σ_{inf}^{OHT}, as in the case of unnotched strength σ^{UNT}, regardless of the presence of the hole, and is defined as

$$\sigma_{inf}^{OHT} = \sigma^{UNT} = \frac{P}{w \cdot t} \tag{2}$$

The latter method is commonly preferred in advanced composite design, such as in the generation of allowable strength values in the aerospace industry. The effect of the presence of the hole is to effectively reduce the value of the maximum load to failure, thus reducing the calculated strength.

All specimens of reference family A are tested to failure, which is selected as the maximum point in the load–deflection curve, and is followed by a catastrophic drop in load carrying capability. Remote strength σ_{inf}^{OHT} (Eq. (2)) is used to generate the plot of Fig. 2, which shows the variation of strength with increasing hole diameter. It should be noted that the ratio of hole diameter to specimen width (D/W) is not held constant for the specimens used to generate Fig. 2, since all specimens are 2.0-in. wide regardless of the hole size. In general, the trend observed is of decreasing strength with increasing hole size, which is to be expected given the reduced section area capable of carrying load. The scatter associated with the data is as high as 26% and is typical of wood-based products.

A rather rare feature of Fig. 2 is that for the smaller hole sizes tested, the majority of the failure locations occurs in the gross section of the specimen, away from the hole. In particular, only 10% of the specimens fail in the net section for the 1/8 in. (3.2 mm) hole diameter, while and even for hole sizes up to 3/4 in. (19 mm) the number of hole failures does not exceed 75%, as shown in Fig. 3. Furthermore, the increase from less than 30% to over 70% is rather rapid, suggesting a clear change in response of the material/specimen combination. This phenomenon is not common in traditional metallic and composite materials, where the stress concentration in proximity of the hole inevitably generates failure in the net section area. Figs. 4 and 5 show typical specimens with failure locations at or away from the hole for several hole sizes.

For isotropic infinite plates containing a circular hole, the increase in stress in the vicinity of the hole can be described by the well-known power law expression of Fig. 6:
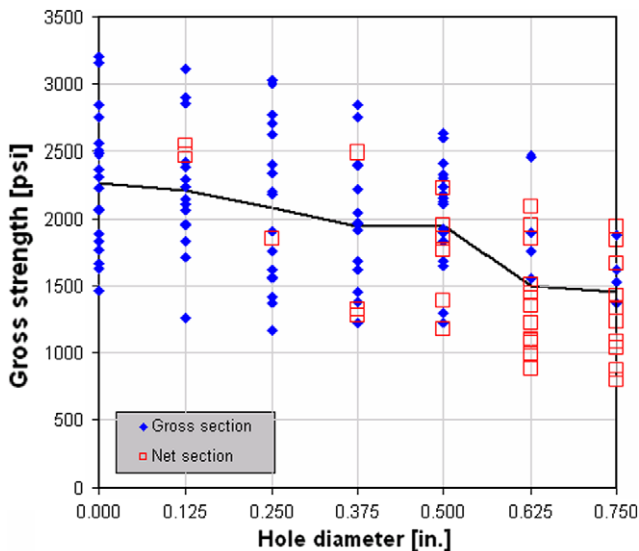

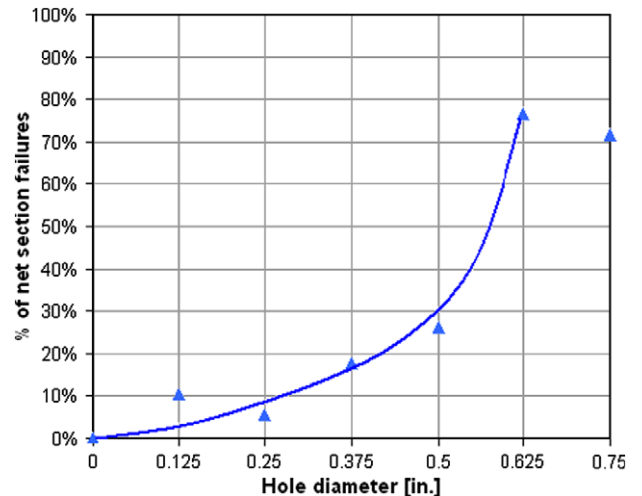**Fig. 2.** Gross section strength variation with hole size for 8 in. × 2 in. (203 mm - 51 mm) specimens.

Fig. 3. Number of specimens that fail at the net section (in % of all specimens tested for a given hole size).
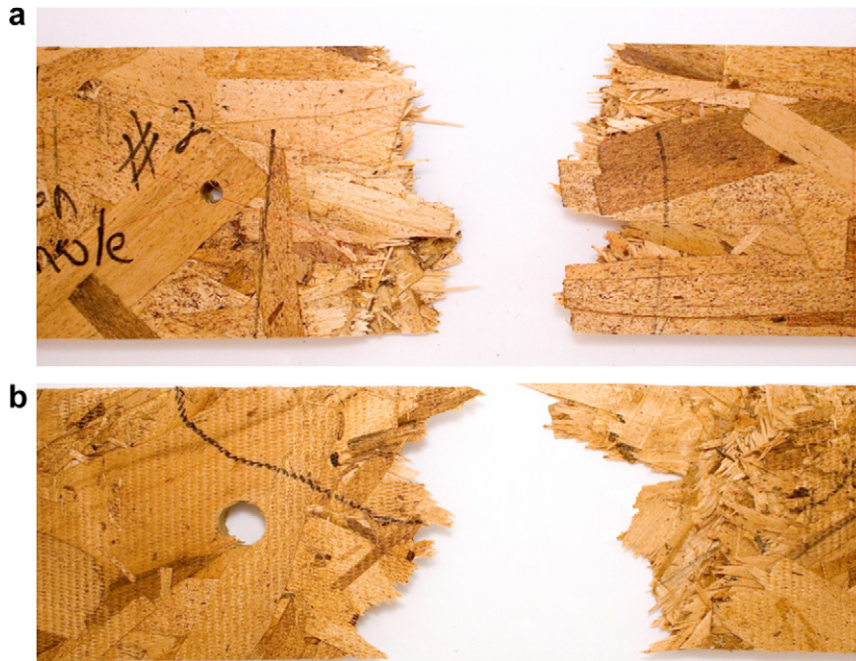
Fig. 4. (a, b) OSB specimens showing failure at the gross section for (top) 0.25 in. (6.35 mm) and (bottom) 0.50 in. (12.7 mm) diameter holes.

$$\sigma_\theta = \frac{1}{2}\sigma\left(1+\frac{a^2}{r^2}\right) - \frac{1}{2}\sigma\left(1+\frac{3a^4}{r^4}\right)\cos(2\theta) \qquad (3)$$

where a is the hole radius, r is the radial distance from the center of the hole, and θ is the angle comprised between r and the loading axis, a can be verified in any fundamental solid mechanics textbook. The point stress criterion, formulated by Whitney and Nuismer [17] to predict the notched strength of advanced polymer composites, relies on the isotropic stress concentration expression and modifies it by introducing the concept of the characteristic dimension d_0. If

we specify the index I as the ratio of applied remote stress σ over the unnotched tensile strength σ^{UNT},

$$I = \frac{\sigma}{\sigma^{UNT}} \qquad (4)$$

the point stress criterion specifies that failure will occur when I reaches the value of unity at a location distant d_0 from the hole, known as characteristic dimension. This d_0 has been shown to be constant for a given material form, material type and stacking sequence for advanced polymer composites.

Fig. 5. (a, b) OSB specimens show failure at the net section for (a) 0.50 in. (12.7 mm) and (b) 0.75 in. (19 mm) diameter holes.
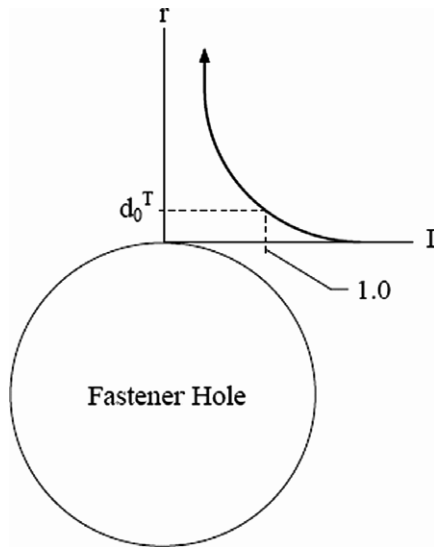
Fig. 6. Schematic describing the point stress criterion and stress concentration around a circular hole.

We can re-write Eq. (3) in terms of variables of interest as

$$\sigma_{OHT} = \frac{2(a+d_o)^4 \sigma_{UNT}}{6a^4 + 10a^3 d_o + 13a^2 d_o^2 + 8a d_o^3 + 2d_o^4} \tag{5}$$

It is then possible to calculate an average value of $d_0 = 0.215$ in. (5.46 mm), as shown in Table 3. The predicted strength is plotted in Fig. 7 against the measured values, and shows good agreement given the already measured variation in the data.

Table 3
Determination of characteristic dimension

Family	Average strength (psi)	Standard deviation (psi)	Do (in.)
0.000	2272.4	501.1	–
0.125	2211.6	435.5	0.226
0.250	2083.5	584.9	0.221
0.375	1946.4	492.0	0.200
0.500	1955.4	413.6	0.306
0.625	1506.4	437.0	0.159
0.750	1450.8	308.2	0.172
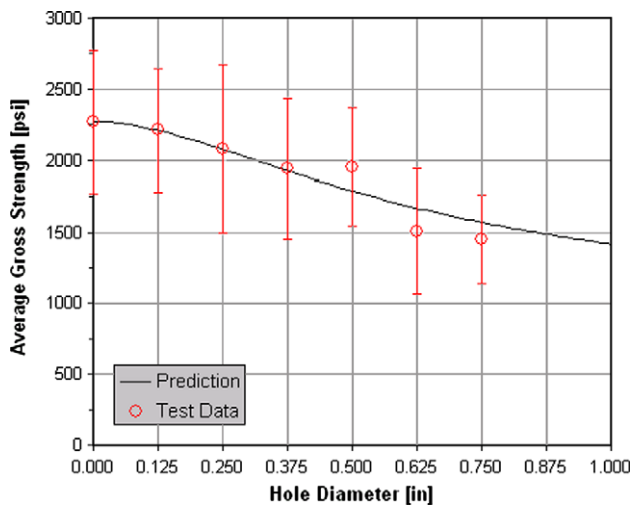
A possible explanation for the phenomena observed can be found in the non-homogenous nature of the OSB wood composite. Its meso-structure (more so than the true micro-structure) is such that the geometric K_t due to the presence of the hole may have less influence on failure than an "inherent material" K_t. The material K_t for non-homogeneous materials, such as short fiber composites, has been attributed [18] to the presence of high stress concentration at the end of the randomly distributed reinforcing fibers. In the case of OSB, the wood strands effectively act as the short reinforcements, and the mismatch in elastic properties between the strand and the surrounding matrix, as well as the neighboring strands that may be oriented in different directions, generates local peak stresses that generate failure. Furthermore, OSB is characterized by the presence of voids and dry spots, and those will also contribute to the local heterogeneity of the material.

Using the characteristic dimension d_0, Waddoups et al. [19] suggested, for advanced polymer composites, that it is possible to calculate the stress concentration factor K_t:

$$K_t = \sqrt{\frac{d+d_0}{d_0}} \tag{6}$$

Referring to Fig. 3, the percentage of failures occurring at the net section exceeds the 50th percentile for a hole diameter between 0.500 in. and 0.625 in. (12.7 mm and 15.9 mm, respectively). For smaller hole diameters, the "inherent material" stress concentration due to the heterogeneous meso-structure is greater than the geometric stress concentration, thus failure occurs mostly at the gross section. If we select the cut-off line at 70% of hole failures, the inherent material stress concentration can be calculated as 2.11 for $D = 0.625$ in. (16.9 mm). This would suggest that only 1/2.11 (or 0.47) of the theoretical strength of a theoretical pristine (parent wood) material could be achieved.

Given the fact that such a high percentage of failures occurs at the gross section even for specimens with large holes, the data in Fig. 2 can be rearranged in Fig. 8 to differentiate the strength calculation according to the failure location. Strength calculation for specimens that effectively fail at the gross section is performed with Eq. (2), while for specimens that fail at the net section Eq. (1) is used. The strength calculation thus employs a selective strength, accounting to the effective failure section area Fig. 8 shows that if the effective failure section is employed, all strength data can be bound by two constant values, around 3200 psi
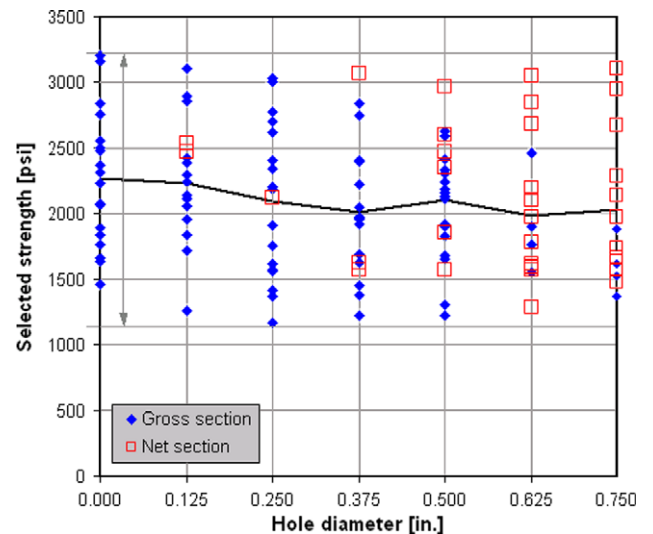

Fig. 7. Predicted strength vs. hole diameter for all configurations tested.

Fig. 8. Selective strength variation with hole size for 2 in. × 8 in. (203 mm × 51 mm) specimens.
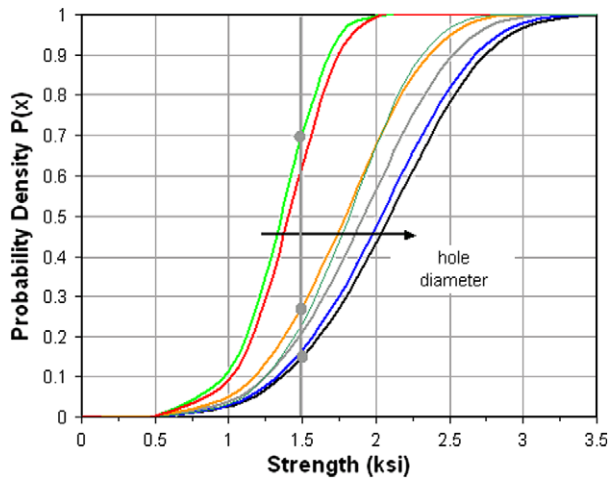
Fig. 9. Strength probability density functions as they vary with hole sizes for the baseline 8 in × 2 in. (203 mm × 51 mm) specimens.

(22.0 MPa) for the upper bound and around 1200 psi (8.3 MPa) for the lower bound, and that it oscillates around an average value of approximately 2100 psi (14.5 MPa), with a coefficient of variation around 23%. The data suggests that the material is notch insensitive, as traditional metallic materials but unlike typical composite materials [20]. This means that the strength value does not vary in the presence of the hole, and furthermore it does not decrease non-linearly for increasing hole sizes.

It should be noted that in the above analysis finite width effects have been neglected, but that given the hole/width ratios considered in this investigation (up to 0.375), the finite width effect might partially influence the results. However, the author is not aware of previous work that has addressed the fracture behavior of OSB, including the validation of classical fracture mechanics correction factors.

Using a two-parameter Weibull distribution, it is possible to plot the probability density functions for all gross strength σ_{inf}^{OHT} data of family A:

$$P(x) = 1 - e^{-\left(\frac{x}{\beta}\right)^{\alpha}} \tag{7}$$

where β is the scale parameter, or the measured strength in ksi, which indicates the location of the distribution, and α is the shape parameter, which measures the spread. For the unnotched specimens, values of $\alpha = 4.43$ and $\beta = 2.27$ best fit the data, while for the largest hole diameter specimens $\alpha = 5.32$ and $\beta = 1.45$. It should be noted that the value of α increases slightly for larger hole sizes, due to a decrease of variation in measured strength. A value of $\alpha = 4.76$ can be calculated as best average fit for the entire set of data points in family A, while the average β can be chosen as 1.91.

These results are in line with those observed for LSL in [15], where a two-parameter Weibull distribution is used to fit the tensile strength data. The measured values range from 4.5 to 3.7 for the shape parameter, and 8.1–3.6 (×1000 psi) for the scale parameter. The greater values are for the fully aligned configuration, while the lower are for the completely random ones, in a fashion similar to OSB. It should be kept in mind that the reinforcement length of LSL can be considered as continuous, while OSB can be considered as a traditional discontinuous fiber composite.

The most significant observation that comes out from Fig. 9 is that the distributions for notched specimens overlap the one of the unnotched specimens, and furthermore that the distribution of several specimens having large holes overlap the distribution of specimens with smaller holes. This observation can provide an explanation for the phenomenon that a large portion of notched specimens does not fail at the hole but rather in the gross section, where the strength of the unnotched material is exceeded.

All results presented so far refer to family A. The hole diameter is varied for constant specimen width, giving rise to varying D/W ratios, and all results are calculated without including the finite width effect. In order to investigate the issues associated with same D/W ratios for varying widths, scaled-up specimens of families B, C and D are tested, both in unnotched and notched configurations. Specimen length is also varied in order to generate geometrically proportional specimens, albeit of constant thickness. In general, for all families tested plots such as the ones in Figs. 2 and 8 can be constructed, reinforcing the previous observation that OSB material is notch insensitive. However, based on the previous observation that for OSB selective strength can be a more relevant indicator of the true material strength than gross strength, remaining constant over varying hole diameters, it may be more significant to plot the variation of average selective strengths against D/W ratios.

Using the average of several measurements for various D/W ratios, and plotting them for each specimen family, it can be seen that although the high variation in the data of Fig. 10 has a tendency to mask the trends, there is a consistent decrease in average strength as specimen size increases (Fig. 11).
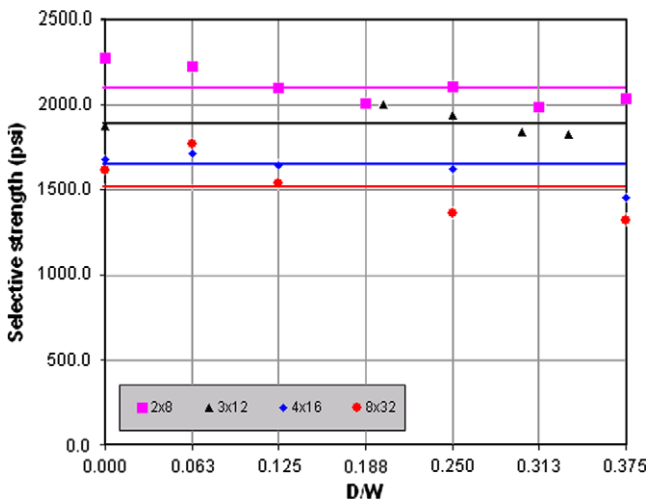

Fig. 10. Selective strength remains constant with increasing D/W ratios for all specimen configurations tested.
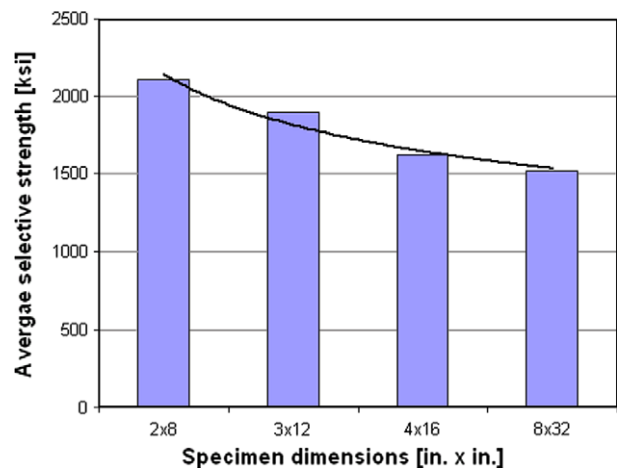

Fig. 11. Variation of the selective strength of Fig. 10 as it decreases between the baseline and the scaled-up specimens.

The decrease of UNT strength with specimen width, although partly consistent with past observations on advanced polymer composites, cannot be explained via first-ply failure and classical laminated plate theory. Furthermore, common analysis methods used for homogenous materials, independent from their isotropic or orthotropic nature, cannot be used to predict notched strength value and location due to the complex stress state in the meso-structure. Therefore, predicting the UNT and OHT strength of OSB wood composites poses a challenge for traditional mechanics, which requires further and careful study, possibly based on damage mechanics. However, this falls beyond the scope of the present paper.

4. Conclusions

For the notched configurations tested, results on OSB wood composites show that the macroscopic response is virtually notch-insensitive, possibly due to the internal stress concentration arising from the heterogeneous nature of the substructure. An "inherent material" stress concentration factor can be derived, and it has been used to explain the tendency of the material to fail at the gross section regardless of the presence of a hole for several hole sizes. There also appears to be a relationship between specimen geometry and measured strength, possibly associated with the finite length scale of the reinforcing strand.

Acknowledgement

References

[1] Youngquist J. Wood-based composites and panel products. Wood handbook-wood as an engineering material, FPL-GTR-113, Forest Products Laboratory (Madison, WI), US Department of Agriculture, Forest Service, 1999 [Chapter 10].

[2] Rebollar M, Perez R, Vidal R. Comparison between oriented strand boards and other wood-based panels for the manufacture of furniture. Mater Des 2007;28(3):882–8.

[3] OSB Design Manual, Structural Board Association, Markham, ON; 2004.

[4] OSB: Performance by design, Structural Board Association, Markham, ON; 2005.

[5] Oudjehane A, Lam F, Avramidis S. Forming and pressing processes of random and oriented wood composite mats. Compos Part B: Eng 1998;29(3):211–5.

[6] Oudjehane A, Lam F. On the density profile within random and oriented wood-based composite panels: horizontal distribution. Compos Part B: Eng 1998;29(6):687–94.

[7] Yadama V, Wolcott MP, Smith LV. Elastic properties of wood-strand composites with undulating strands. Compos Part A: Appl Sci Manuf 2006;37(3):385–92.

[8] Nishimura T, Ansell MP, Ando N. Prediction of oriented strand board properties from mat formation and compression operating conditions. Part 1. Horizontal density distribution and vertical density profile. Wood Sci Technol 2006;40(2):139–58.

[9] Painter G, Budman H, Pritzker M. Prediction of oriented strand board properties from mat formation and compression operating conditions. Part 2: MOE prediction and process optimization. Wood Sci Technol 2006;40(4):291–307.

[10] Nishimura T, Ansell MP, Ando N. Evaluation of the arrangement of wood strands at the surface of OSB by image analysis. Wood Sci Technol 2002;36(1):93–9.

[11] Nishimura T, Amin J, Ansell MP. Image analysis and bending properties of model OSB panels as a function of strand distribution, shape and size. Wood Sci Technol 2004;38(4):297–309.

[12] Nishimura T, Ansell MP. Monitoring fiber orientation in OSB during production using filtered image analysis. Wood Sci Technol 2002;36(3):229–39.

[13] Nishimura T, Ansell MP, Ando N. The relationship between the arrangement of wood strands at the surface of OSB and the modulus of rupture determined by image analysis. Wood Sci Technol 2003;35(6):555–62.

[14] Thomas W. Poisson's ratios of an oriented strand board. Wood Sci Technol 2003;37(3–4):259–68.

[15] Moses DM, Prion HGL, Li W, Boehner W. Composite behavior of laminated strand lumber. Wood Sci Technol 2003;37(1):59–77.

[16] SRM 5R-94, Open-hole tensile properties of oriented fiber–resin composites, Suppliers of advanced composites manufacturing association (SACMA) recommended methods, Composites fabricators association (CFA); 1999.

[17] Whitney JM, Nuismer RJ. Stress fracture criteria for laminated composites containing stress concentrations. J Comp Mater 1974;8:253–65.

[18] Kardos JL, Michno MJ, Duffy TA. Investigation of high performance short fiber reinforced plastics. Final Report, Naval Air Systems Command, No. N00019-73-C-0358; 1974.

[19] Waddoups ME, Eisenmann JR, Kaminski BE. Macroscopic fracture mechanics of advanced composite materials. J Compos Mater 1971;5:446–54.

[20] Whitney J. Fracture analysis of laminates. Engineered materials handbook. Composites, vol. 1. ASM International; 1987.